

# Updated reduced CMB data and constraints on cosmological parameters

Rong-Gen Cai<sup>1,2,\*</sup> Zong-Kuan Guo<sup>1,†</sup> and Bo Tang<sup>1‡</sup>

<sup>1</sup> *State Key Laboratory of Theoretical Physics,  
Institute of Theoretical Physics, Chinese Academy of Sciences,  
P.O. Box 2735, Beijing 100190, China*

<sup>2</sup> *King Abdulaziz University, Jeddah 21589, Saudi Arabia*

(Dated: June 6, 2019)

## Abstract

We obtain the reduced CMB data  $\{l_A, R, z_*\}$  from WMAP9, WMAP9+BICEP2, Planck+WP and Planck+WP+BICEP2 for the  $\Lambda$ CDM and  $w$ CDM models with or without spatial curvature. We then use these reduced CMB data in combination with low-redshift observations to put constraints on cosmological parameters. We find that including BICEP2 results in a higher value of the Hubble constant especially when the equation of state of dark energy and curvature are allowed to vary. For the  $\Lambda$ CDM model with curvature, the estimate of the Hubble constant with Planck+WP+Lensing is inconsistent with the one derived from Planck+WP+BICEP at about 1.3  $\sigma$  confidence level.

---

\*Electronic address: cairg@itp.ac.cn

†Electronic address: guozk@itp.ac.cn

‡Electronic address: tangbo@itp.ac.cn

## I. INTRODUCTION

Since the discovery of the cosmic acceleration expansion of the universe based on the distance measurement of type Ia Supernovae (SNe Ia) [1, 2], its origin has become a hot topic in modern cosmology and theoretical physics. The cause to the observed cosmic acceleration is due to the so-called dark energy with negative pressure in general relativity framework, or the modification to general relativity at cosmic scales.

To study properties of dark energy, one may combine some mature probes, such as SNe Ia, the observational Hubble parameter (HUB), baryon acoustic oscillation (BAO) and cosmic microwave background (CMB) anisotropy. The SNe Ia, HUB and BAO probe the expansion of the universe at low and intermediate redshifts, while the CMB measurements probe the distance at high-redshift (especially the distance to the surface of last-scattering). The CMB data provide the strongest constraints on cosmological parameters [3] and help break the degeneracies among the dark energy and other cosmological parameters.

The reduced CMB data  $\{l_A, R, z_*\}$  provide an efficient summary of CMB information, of which  $l_A$  is the angular scale of the sound horizon at recombination and determines the acoustic peak structure of the CMB angular power spectra,  $R$  is the scaled distance to the recombination and determines the amplitude of the acoustic peak and  $z_*$  is the redshift at the last scattering surface. Instead of the full CMB spectra, the reduced CMB data relating the distance to the last scattering surface provide a fast and self-consistent approach for combining the CMB information with complementary cosmological data to constrain late-time cosmological parameters. The reduced CMB data are firstly derived in [4] from the three-year WMAP data for the  $\Lambda$ CDM model (with and without spatial curvature) and they find that dark energy density is consistent with a constant in cosmic time and a flat universe is allowed by using the reduced CMB data together with the SNe Ia and BAO data. Recently Wang and Wang [5] obtained the reduced CMB data from WMAP9 and Planck+WP+Lensing for the  $\Omega_k+\Lambda$ CDM model and found that the reduced CMB data derived from Planck+WP+Lensing are much tighter than those from WMAP9, but when combined with other low-redshift observational data, the reduced CMB data do not improve the constraints on the dark energy too much compared to those from WMAP9. More recently, Shafer and Huterer [6] derived the reduced CMB data from WMAP9 and Planck+WP respectively for the flat  $w$ CDM model, when combining the reduced CMB

data, BAO and 3 samples of SNe Ia data (Union2.1 [7], SNLS3 [8] and PS1 [9]) respectively, they found that there is a preference for the equation of state of dark energy  $w < -1$  for the constraints with Planck but not with WMAP9. There are many works that use the reduced CMB data together with complementary cosmological data to constrain late-time cosmology [10–13].

There are two advantages of the reduced CMB data. First, the CMB shift parameters  $l_A$  and  $R$  together with the decoupling redshift  $z_*$ , extracted from the CMB angular power spectra, allow one to quickly evaluate the likelihood of various dark energy models, without the need to run a Markov Chain Monte Carlo exploration of the CMB likelihood which usually includes a number of astrophysical parameters to describe unresolved foreground components and other nuisance parameters. Second, it provides an efficient and appropriate summary of CMB data as far as dark energy constraints are concerned. Since  $l_A$  determines the acoustic structure in CMB angular power spectra while  $R$  determines the overall amplitude of the acoustic peaks, they are nearly uncorrelated. Both  $R$  and  $l_A$  can be used to further compress CMB information and combined with other measurements in a friendly user manner to constrain dark energy models.

On the other hand, the authors of [14] analyzed the likelihood of the reduced CMB data with WMAP3 data for the base  $\Lambda$ CDM model involving extra parameters, such as tensor modes and a running spectral index. They found that adding curvature or slightly modifying the dark energy parameters does not significantly change the values of  $\{l_A, R\}$ , which, however, change large when more parameters like tensor modes or running of the scalar spectral index are involved.

The purposes of this work are to update constraints on the parameter combination  $\{l_A, R, z_*\}$  using newly released CMB temperature and polarization data for several cosmological models and to test their dependence on model assumptions. These updated reduced CMB data provide a simple and efficient method for combining in a friendly user manner the current CMB measurements with low redshift data. We first obtain the reduced CMB data from WMAP9 data [15] and Planck data [16] together with WMAP polarization data (WP), based on the  $\Lambda$ CDM model and  $w$ CDM model with a flat or curved space curvature, respectively. We also combine the newly released BICEP2 polarization data [17] to derive the reduced CMB data. Our goal is to see the differences among the data used when combine the reduced CMB data with the low redshift observational data to constrain different

cosmological models.

The paper is organized as follows. In section II we present the reduced CMB data obtained from WMAP9, Planck+WP, Planck+WP+BICEP2 and WMAP9+BICEP2 based on different cosmological models, respectively. In section III we give the results of the combination of reduced CMB data and other data sets to constrain the different cosmological models. The conclusions are included in section IV.

## II. REDUCED CMB DATA

The distance measurement is one of the most powerful methods to study the evolution history of the universe. In a Friedmann-Robertson-Walker universe, the comoving distance from an observer to redshift  $z$  is given by

$$\begin{aligned} r(z) &= H_0^{-1} |\Omega_k|^{-1/2} \text{sinn}[|\Omega_k|^{-1/2} \Gamma(z)], \\ \Gamma(z) &= \int_0^z \frac{dz'}{E(z')}, \quad E(z) = H(z)/H_0, \end{aligned} \quad (1)$$

where  $\Omega_k = -k/H_0^2$  ( $k$  is the spatial curvature constant) and  $\text{sinn}(x) = \sin(x)$ ,  $x$ ,  $\sinh(x)$  for  $\Omega_k < 0$ ,  $\Omega_k = 0$ , and  $\Omega_k > 0$ , respectively. The Hubble parameter is given by the Friedmann equation

$$\begin{aligned} H^2(z) &= H_0^2 [\Omega_{r0}(1+z)^4 + \Omega_{dm0}(1+z)^3 + \Omega_{b0}(1+z)^3 + \\ &\quad \Omega_k(1+z)^2 + (1 - \Omega_{m0} - \Omega_{r0} - \Omega_k)], \end{aligned} \quad (2)$$

for the  $\Lambda$ CDM model, where the redshift  $z$  is defined by  $(1+z) = 1/a$ , and  $\Omega_{r0}$ ,  $\Omega_{dm0}$  and  $\Omega_{b0}$  are the present values of the fraction energy density for radiation, dark matter and baryon matter, respectively. The latter two are often written as the total matter density  $\Omega_{m0} = \Omega_{b0} + \Omega_{dm0}$ . The radiation density is the sum of photons and relativistic neutrinos [15]:

$$\Omega_{r0} = \Omega_\gamma^{(0)}(1 + 0.2271N_{eff}), \quad (3)$$

where  $N_{eff} = 3.046$  is the effective number of neutrino species in the Standard Model of particle physics [18], and  $\Omega_\gamma^{(0)} = 2.469 \times 10^{-5} h^{-2}$  for  $T_{\text{CMB}} = 2.725K$  ( $h \equiv H_0/100 \text{ km s}^{-1} \text{ Mpc}^{-1}$ ). For the  $w$ CDM model, the Hubble parameter is given by

$$\begin{aligned} H^2(z) &= H_0^2 [\Omega_{r0}(1+z)^4 + \Omega_{dm0}(1+z)^3 + \Omega_{b0}(1+z)^3 + \\ &\quad \Omega_k(1+z)^2 + (1 - \Omega_{m0} - \Omega_{r0} - \Omega_k)F(z)], \end{aligned} \quad (4)$$

where the evolving function  $F(z)$ , depending on the equation of state of dark energy, is given by

$$F(z) = (1+z)^{3+3w}. \quad (5)$$

It is noticed that here we have not assumed a flat universe model. As for a flat universe, the curvature terms disappear in equation (2) and equation (4) since  $\Omega_k = 0$ . There are four cases considered here, which are the  $\Lambda$ CDM model and the  $w$ CDM model with a flat and curved space curvature, respectively.

Data	flat $\Lambda$ CDM	$\Omega_k + \Lambda$ CDM	flat $w$ CDM	$\Omega_k + w$ CDM
WMAP9	this work	Ref. [5]	Ref. [6]	Ref. [15]
PLANCK+WP	this work	Ref. [5] (+Lensing)	Ref. [6]	this work
PLANCK+WP+BICEP2	this work	this work	this work	this work
WMAP9+BICEP2	this work	this work	this work	this work

Table 1: References for the reduced CMB data derived from different CMB data in different cosmological models.

In the CMB measurement, the distance to the last scattering surface can be accurately determined from the locations of peaks and troughs of acoustic oscillations. There are two quantities: one is the ‘‘acoustic scale’’

$$l_A = (1+z_*) \frac{\pi D_A(z_*)}{r_s(z_*)}, \quad (6)$$

and the other is the ‘‘shift parameter’’

$$R = \sqrt{\Omega_{m0} H_0^2} (1+z_*) D_A(z_*). \quad (7)$$

Here  $D_A(z) = r(z)/(1+z)$  is the angular diameter distance and  $z_*$  is the redshift at the last scattering surface [19]

$$z_* = 1048[1 + 0.00124(\Omega_{b0} h^2)^{-0.738}][1 + g_1(\Omega_{m0} h^2)^{g_2}], \quad (8)$$

where

$$g_1 = \frac{0.0783(\Omega_{b0} h^2)^{-0.238}}{1 + 39.5(\Omega_{b0} h^2)^{0.763}}, \quad (9)$$

$$g_2 = \frac{0.560}{1 + 21.1(\Omega_{b0} h^2)^{1.81}}.$$

Data	$l_A \pm \sigma$	$R \pm \sigma$	$z_* \pm \sigma$	Correlation Matrix
WMAP9	$301.95 \pm 0.66$	$1.7257 \pm 0.0165$	$1088.96 \pm 0.84$	1.0000 0.3859 0.4998 0.3859 1.0000 0.8432 0.4998 0.8432 1.0000
PLANCK+WP	$301.66 \pm 0.18$	$1.7500 \pm 0.0089$	$1090.33 \pm 0.53$	1.0000 0.5126 0.4552 0.5126 1.0000 0.8699 0.4552 0.8699 1.0000
PLANCK+WP +BICEP2	$301.61 \pm 0.18$	$1.7474 \pm 0.0091$	$1089.91 \pm 0.55$	1.0000 0.5567 0.4975 0.5567 1.0000 0.8542 0.4975 0.8442 1.0000
WMAP9+BICEP2	$301.63 \pm 0.66$	$1.7263 \pm 0.0222$	$1088.95 \pm 1.26$	1.0000 0.4424 0.5028 0.4424 1.0000 0.9294 0.5028 0.9294 1.0000

Table 2: The mean values, standard deviations of  $\{l_A, R, z_*\}$  and the correlation matrix for the flat  $\Lambda$ CDM model.

These quantities can be used to constrain some cosmological parameters without need to use the full likelihoods of WMAP9 [15] or Planck data [16].

Based on the original idea proposed in [4], Hinshaw *et al.* [15] obtained constraints on the parameter combination  $\{l_A, R, z_*\}$  from WMAP9 data based on the  $w$ CDM model without assuming a flat universe. Wang and Wang [5] obtained the mean values and normalized covariance matrix of  $\{l_A, R, \Omega_{b0}h^2, n_s\}$  from WMAP9 and Planck+WP+Lensing data, respectively, based on the  $\Omega_k+\Lambda$ CDM model. Recently, Shafer and Huterer [6] derived the related results about  $\{l_A, R, z_*\}$  from WMAP9 and Planck+WP data, respectively, based on the flat  $w$ CDM model. In this section, following Wang and Wang [5] we obtain the Markov chains using the Markov Chain Monte Carlo sampler as implemented in the CosmoMC package [20] and then derive constraints on the parameter combination  $\{l_A, R, z_*\}$ . In our analysis, we focus on four cosmological models listed in Table 1, based on the six-parameter model in the case of the flat  $\Lambda$ CDM model, described by

$$\{\Omega_{b0}h^2, \Omega_{dm0}h^2, \Theta_s, \tau, A_s, n_s\},$$

Data	$l_A \pm \sigma$	$R \pm \sigma$	$z_* \pm \sigma$ or $w_b \pm \sigma$	Correlation Matrix									
WMAP9	$302.02 \pm 0.66$	$1.7327 \pm 0.0164$	$0.02260 \pm 0.00053$	<table border="1"> <tr> <td>1.0000</td> <td>0.3883</td> <td>-0.6089</td> </tr> <tr> <td>0.3883</td> <td>1.0000</td> <td>-0.5239</td> </tr> <tr> <td>-0.6089</td> <td>-0.5239</td> <td>1.0000</td> </tr> </table>	1.0000	0.3883	-0.6089	0.3883	1.0000	-0.5239	-0.6089	-0.5239	1.0000
1.0000	0.3883	-0.6089											
0.3883	1.0000	-0.5239											
-0.6089	-0.5239	1.0000											
PLANCK+WP +Lensing	$301.57 \pm 0.18$	$1.7407 \pm 0.0094$	$0.02228 \pm 0.00030$	<table border="1"> <tr> <td>1.0000</td> <td>0.5250</td> <td>-0.4475</td> </tr> <tr> <td>0.5250</td> <td>1.0000</td> <td>-0.6925</td> </tr> <tr> <td>-0.4475</td> <td>-0.6925</td> <td>1.0000</td> </tr> </table>	1.0000	0.5250	-0.4475	0.5250	1.0000	-0.6925	-0.4475	-0.6925	1.0000
1.0000	0.5250	-0.4475											
0.5250	1.0000	-0.6925											
-0.4475	-0.6925	1.0000											
PLANCK+WP +BICEP2	$301.48 \pm 0.19$	$1.7352 \pm 0.0100$	$1089.14 \pm 0.61$	<table border="1"> <tr> <td>1.0000</td> <td>0.5992</td> <td>0.5479</td> </tr> <tr> <td>0.5992</td> <td>1.0000</td> <td>0.8801</td> </tr> <tr> <td>0.5479</td> <td>0.8801</td> <td>1.0000</td> </tr> </table>	1.0000	0.5992	0.5479	0.5992	1.0000	0.8801	0.5479	0.8801	1.0000
1.0000	0.5992	0.5479											
0.5992	1.0000	0.8801											
0.5479	0.8801	1.0000											
WMAP9+BICEP2	$301.69 \pm 0.66$	$1.7170 \pm 0.0243$	$1088.51 \pm 1.36$	<table border="1"> <tr> <td>1.0000</td> <td>0.4301</td> <td>0.4994</td> </tr> <tr> <td>0.4301</td> <td>1.0000</td> <td>0.9407</td> </tr> <tr> <td>0.4994</td> <td>0.9407</td> <td>1.0000</td> </tr> </table>	1.0000	0.4301	0.4994	0.4301	1.0000	0.9407	0.4994	0.9407	1.0000
1.0000	0.4301	0.4994											
0.4301	1.0000	0.9407											
0.4994	0.9407	1.0000											

Table 3: The mean values, standard deviations of  $\{l_A, R, z_*\}$  and the correlation matrix for the  $\Omega_k + \Lambda$ CDM model.

where  $\Theta_s$  is the ratio of the sound horizon to the angular diameter distance at the photon decoupling,  $\tau$  is the Thomson scattering optical depth due to reionization,  $A_s$  is the amplitude of primordial curvature perturbations and  $n_s$  is the scalar spectral index. The CMB data sets used in our analysis are listed in Table 1. Here we emphasize that both the tensor-to-scalar ratio  $r$  and running of the scalar spectral index  $\alpha_s$  are allowed to vary if the BICEP2  $B$ -mode polarization data are included, because the  $B$ -mode power spectrum from the BICEP2 experiment implies the detect of primordial gravitational wave at  $7.0 \sigma$  ignoring foreground dust [17] and allowing the running of the scalar spectral index reconciles the tension with the Planck constraints on  $r$  [21]. It is argued in [22, 23] that given the uncertainties of the amplitude of the dust polarization at the BICEP2 frequency of 150 GHz one cannot say conclusively at present whether the B-modes detected by BICEP2 are due to gravity waves or just polarized dust. In [26] using genus statistics they find evidence for a detection of a gravity wave signal with  $r = 0.11 \pm 0.04$ . Recently, Planck team releases polarization data from 100 to 353 GHz. Extrapolation of the Planck 353 GHz data to 150 GHz gives a dust power, which is the same magnitude as reported by BICEP2 [24].

Data	$l_A \pm \sigma$	$R \pm \sigma$	$z_* \pm \sigma$	Correlation Matrix
WMAP9	$301.98 \pm 0.66$	$1.7302 \pm 0.0169$	$1089.09 \pm 0.89$	1.0000 0.4077 0.5132 0.4077 1.0000 0.8580 0.5132 0.8580 1.0000
PLANCK+WP	$301.65 \pm 0.18$	$1.7499 \pm 0.0088$	$1090.41 \pm 0.53$	1.0000 0.5262 0.4708 0.5262 1.0000 0.8704 0.4708 0.8704 1.0000
PLANCK+WP +BICEP2	$301.60 \pm 0.18$	$1.7466 \pm 0.0089$	$1089.87 \pm 0.53$	1.0000 0.5256 0.4597 0.5256 1.0000 0.8422 0.4597 0.8422 1.0000
WMAP9+BICEP2	$301.71 \pm 0.67$	$1.7292 \pm 0.0229$	$1089.15 \pm 1.32$	1.0000 0.4466 0.5119 0.4466 1.0000 0.9332 0.5119 0.9332 1.0000

Table 4: The mean values, standard deviations of  $\{l_A, R, z_*\}$  and the correlation matrix for the flat  $w$ CDM model.

However, if more than one dusty region is present along the line-of-sight, with even mildly different temperature and dust column density, but severely misaligned magnetic field, then the validity of such an extrapolation breaks down [25].

The mean values, the standard deviations and their correlation matrix of  $\{l_A, R, z_*\}$  (or  $\{l_A, R, \Omega_{b0}h^2\}$ ) for four cosmological models by using different data are summarized in Table 2 to Table 5, respectively. It is noticed that Wang and Wang [5] used  $\Omega_{b0}h^2$  instead of  $z_*$ , which gives identical constraints by replacing  $\Omega_{b0}h^2$  with  $z_*$ . Different from other cases in the third row of Table 1, they also used Planck data together with Planck lensing.

From Table 2 to Table 5, we see that the Planck data give tighter constraints on  $\{l_A, R, z_*\}$  than WMAP9 in the same cosmological model. Including the BICEP2 data does not change the results significantly but the standard deviations seem to be larger, this is because the running of the scalar spectral index for the power spectrum of scalar perturbations has been added when we use Planck+WP+BICEP2 to obtain constraints on  $\{l_A, R, z_*\}$ . We also notice that there is some tension between the WMAP9 data and Planck data constraining on  $\{l_A, R, z_*\}$ . For example, in Table 2 the constraints on  $R$  ( $z_*$ ) are inconsistent at

Data	$l_A \pm \sigma$	$R \pm \sigma$	$z_* \pm \sigma$	Correlation Matrix
WMAP9	$302.40 \pm 0.67$	$1.7246 \pm 0.0183$	$1090.88 \pm 1.00$	1.0000 0.4262 0.5391 0.4262 1.0000 0.8643 0.5391 0.8643 1.0000
PLANCK+WP	$301.60 \pm 0.18$	$1.7442 \pm 0.0093$	$1089.86 \pm 0.58$	1.0000 0.5698 0.5248 0.5698 1.0000 0.8889 0.5248 0.8889 1.0000
PLANCK+WP +BICEP2	$301.46 \pm 0.19$	$1.7345 \pm 0.0103$	$1089.09 \pm 0.62$	1.0000 0.5922 0.5382 0.5922 1.0000 0.8879 0.5382 0.8879 1.0000
WMAP9+BICEP2	$301.71 \pm 0.68$	$1.7162 \pm 0.0231$	$1088.45 \pm 1.28$	1.0000 0.4017 0.4781 0.4017 1.0000 0.9313 0.4781 0.9313 1.0000

Table 5: The mean values, standard deviations of  $\{l_A, R, z_*\}$  and the correlation matrix for the  $\Omega_k+w$ CDM model.

about  $1.5 \sigma$  ( $1.6 \sigma$ ) when using WMAP9 and Planck+WP. The estimates of  $\{l_A, R, z_*\}$  are consistent with each other within  $1 \sigma$  for the  $\Lambda$ CDM model when we use Planck+WP and Planck+WP+BICEP2 data.

Moreover, the difference of values of the reduced CMB data derived from same data for different models is not significant. As stated in Ref. [14], curvature or slightly modifying the dark energy parameters does not significantly change the values of  $\{l_A, R\}$ . For example, from Table 2 and Table 3 we find that the WMAP9 data give values of  $\{l_A, R\} = \{301.95 \pm 0.66, 1.7257 \pm 0.0165\}$  ( $\{302.02 \pm 0.66, 1.7327 \pm 0.0164\}$ ) for the  $\Lambda$ CDM model without (with) spatial curvature which shows no significant difference.

### III. COSMOLOGICAL PARAMETERS

In the previous section we have derived the reduced CMB data from WMAP9, Planck+WP, Planck+WP+BICEP2 and WMAP9+BICEP2 for the  $\Lambda$ CDM model and the  $w$ CDM model with and without space curvature, respectively. In this section, we focus on

constraints on the cosmological parameters for the corresponding cosmological models from reduced CMB data in combination with the low-redshift observational data including the Union2.1 SNe Ia sample, Hubble parameter and BAO data, which are described in Appendix. The best-fitted values of  $\Omega_{m0}$  and  $h$  for the  $\Lambda$ CDM model,  $\Omega_{m0}$ ,  $h$  and  $w$  for the  $w$ CDM model and their 68% confidence level (CL) errors are given by using the Markov Chain Monte Carlo analysis in the multidimensional parameter space in a Bayesian framework. The results are summarized in Table 6 to Table 9, and their likelihoods are shown in Figure 1 to Figure 4, respectively.

From Table 6 we see that in the context of the flat  $\Lambda$ CDM model, the combination of Planck data favors a relatively higher value of  $\Omega_{m0}$  and a lower value of  $h$  compared to the combination of WMAP9 data. However, the reduced CMB data from Planck+WP do not lead to significantly improve the constraint on dark energy together with low-redshift observational data, compared to the reduced CMB data from WMAP9 even though the Planck measures all of the CMB distance parameters  $\{l_A, R, z_*\}$  more precisely, whose errors are 2 – 3 times smaller. This is because the Planck data appear to favor a higher value of  $\Omega_{m0}$  and a lower value of  $H_0$  in the standard six-parameter  $\Lambda$ CDM model, which are in tension with the magnitude-redshift relation for SNe Ia and recent direct measurements of  $H_0$  [16]. The constraints with BICEP2 data suppress the value of  $\Omega_{m0}$  and raise the value of  $h$ . The tendency seems to appear in all the cosmological models we are considering here. These estimates of  $\Omega_{m0}$  and  $h$  are consistent with each other within 1  $\sigma$  CL, but are in tension with the results derived by Planck [16].

As we can see from Table 7, in the context of  $\Lambda$ CDM model with space curvature, the constraints with Planck+WP+Lensing give  $h = 0.6880_{-0.0096}^{+0.0090}$ , which is inconsistent with the value  $h = 0.7032_{-0.0113}^{+0.0106}$  derived from Planck+WP+BICEP2 at about 1.3  $\sigma$  CL. The Planck group gives  $h = 0.6794$  from Planck+Lensing+WP+highL and  $h = 0.6715$  from Planck+WP+highL, and the value of  $h$  may be enhanced by Planck lensing data [16], so we can conclude that the constraints with Planck+WP in the  $\Lambda$ CDM model with space curvature may give a lower value of  $h$ , which deviates more from  $h = 0.7032$ . Furthermore, the WMAP9 data favor a positive  $\Omega_k$  (an open universe), but the Planck data give a negative  $\Omega_k$  (a closed universe) and the value of  $\Omega_k$  is depressed with the combination of BICEP2 data. However, there is no evidence for any departure from a spatially flat geometry in these three cases.

A cosmological constant has an equation of state (EOS)  $w = -1$ . If we release the EOS  $w$  of dark energy, the constraints with Planck+WP give  $w = -1.0507^{+0.0469}_{-0.0507}$ , as shown in Table 8, which favors the phantom region at  $1 \sigma$  CL. The combination with BICEP2 data gives a relatively higher value of  $w$  ( $w = -1.0426^{+0.0502}_{-0.0539}$ ) while the constraints with WMAP9 (WMAP9+BICEP2) give  $w = -1.0180^{+0.0535}_{-0.0667}$  ( $w = -1.0277^{+0.0666}_{-0.0606}$ ). All the three cases are consistent with the  $\Lambda$ CDM model.

WMAP9, Planck+WP, Planck+WP+BICEP2 and WMAP9+BICEP2 all give negative  $\Omega_k$  (a closed universe) for the  $\Omega_k + w$ CDM model, as shown in Table 9, but are consistent with a flat geometry within  $1 \sigma$  CL.

We also use three sets of the reduced CMB data from Planck+WP+BICEP2 derived from flat  $\Lambda$ CDM,  $\Omega_k + \Lambda$ CDM and  $\Omega_k + w$ CDM, respectively together with the low-redshift observational data to constrain the  $\Omega_k + w$ CDM model. The purpose is to see whether the constraints on the cosmological parameters are sensitive to the choice of the reduced CMB data derived from different cosmological models. Their likelihoods are shown in Figure 5. It is shown that the likelihoods in the three cases are almost the same for each cosmological parameter, which means that the constraints on the cosmological parameters are not sensitive to the choice of the reduced CMB data derived from different cosmological models.

Data	$\Omega_{m0}$	$h$
WMAP9	$0.2877^{+0.0111}_{-0.0110}$	$0.7022^{+0.0110}_{-0.0095}$
Planck+WP	$0.2967^{+0.0106}_{-0.0099}$	$0.6975^{+0.0076}_{-0.0087}$
Planck+WP+BICEP2	$0.2956^{+0.0100}_{-0.0094}$	$0.6998^{+0.0088}_{-0.0092}$
WMAP9+BICEP2	$0.2892^{+0.0117}_{-0.0132}$	$0.7027^{+0.0111}_{-0.0104}$

Table 6: Constraints with  $1 \sigma$  errors on  $\Omega_{m0}$  and  $h$  for the flat  $\Lambda$ CDM model from SNe Ia, HUB, BAO and reduced CMB data.

Data	$\Omega_{m0}$	$h$	$\Omega_k$
WMAP9	$0.2946^{+0.0114}_{-0.0112}$	$0.6904^{+0.0112}_{-0.0126}$	$0.0007^{+0.0051}_{-0.0063}$
Planck+WP+Lensing	$0.2986^{+0.0129}_{-0.0134}$	$0.6880^{+0.0090}_{-0.0096}$	$-0.0006^{+0.0054}_{-0.0067}$
Planck+WP+BICEP2	$0.2948^{+0.0152}_{-0.0121}$	$0.7032^{+0.0106}_{-0.0113}$	$-0.0017^{+0.0063}_{-0.0058}$
WMAP9+BICEP2	$0.2915^{+0.0139}_{-0.0137}$	$0.6983^{+0.0120}_{-0.0125}$	$-0.0012^{+0.0071}_{-0.0075}$

Table 7: Constraints with  $1\sigma$  errors on  $\Omega_{m0}$ ,  $h$  and  $\Omega_k$  for the  $\Omega_k+\Lambda$ CDM model from SNe Ia , HUB, BAO and reduced CMB data.

Data	$\Omega_{m0}$	$h$	$w$
WMAP9	$0.2878^{+0.0116}_{-0.0101}$	$0.7043^{+0.0134}_{-0.0116}$	$-1.0180^{+0.0535}_{-0.0667}$
Planck+WP	$0.2936^{+0.0103}_{-0.0110}$	$0.7048^{+0.0123}_{-0.0104}$	$-1.0507^{+0.0469}_{-0.0507}$
Planck+WP+BICEP2	$0.2919^{+0.0098}_{-0.0104}$	$0.7070^{+0.0109}_{-0.0114}$	$-1.0426^{+0.0502}_{-0.0539}$
WMAP9+BICEP2	$0.2885^{+0.0118}_{-0.0130}$	$0.7054^{+0.0135}_{-0.0141}$	$-1.0277^{+0.0666}_{-0.0606}$

Table 8: Constraints with  $1\sigma$  errors on  $\Omega_{m0}$ ,  $h$  and  $w$  for the flat  $w$ CDM model from SNe Ia , HUB, BAO and reduced CMB data.

Data	$\Omega_{m0}$	$h$	$w$	$\Omega_k$
WMAP9	$0.2963^{+0.0163}_{-0.0160}$	$0.7007^{+0.0232}_{-0.0192}$	$-1.0536^{+0.0791}_{-0.0720}$	$-0.0091^{+0.0104}_{-0.0129}$
Planck+WP	$0.2945^{+0.0162}_{-0.0160}$	$0.7078^{+0.0153}_{-0.0174}$	$-1.0614^{+0.0833}_{-0.0740}$	$-0.0013^{+0.0070}_{-0.0090}$
Planck+WP+BICEP2	$0.2947^{+0.0196}_{-0.0158}$	$0.7142^{+0.0159}_{-0.0190}$	$-1.0661^{+0.0867}_{-0.0724}$	$-0.0050^{+0.0084}_{-0.0081}$
WMAP9+BICEP2	$0.2932^{+0.0161}_{-0.0132}$	$0.7146^{+0.0226}_{-0.0213}$	$-1.0423^{+0.0724}_{-0.0723}$	$-0.0095^{+0.0131}_{-0.0134}$

Table 9: Constraints with  $1\sigma$  errors on  $\Omega_{m0}$ ,  $h$ ,  $w$  and  $\Omega_k$  for the  $\Omega_k+w$ CDM model from SNe Ia, HUB, BAO and reduced CMB data.

#### IV. CONCLUSIONS

The reduced CMB data provide an efficient summary of CMB information, and can be used to constrain cosmological parameters instead of the full CMB power spectra. We have obtained the reduced CMB data from WMAP9 data and Planck data based on the  $\Lambda$ CDM model and  $w$ CDM model with a flat or curved space curvature, respectively. We have also

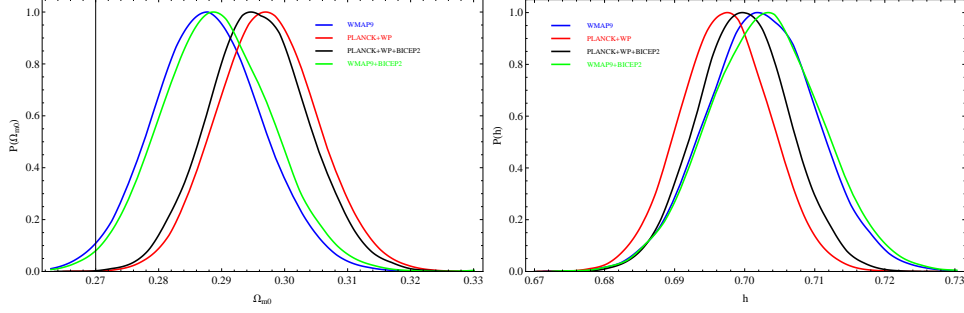


Fig. 1: Marginalized posterior distributions for  $h$  (right) and  $\Omega_{m0}$  (left) of the  $\Lambda$ CDM model.

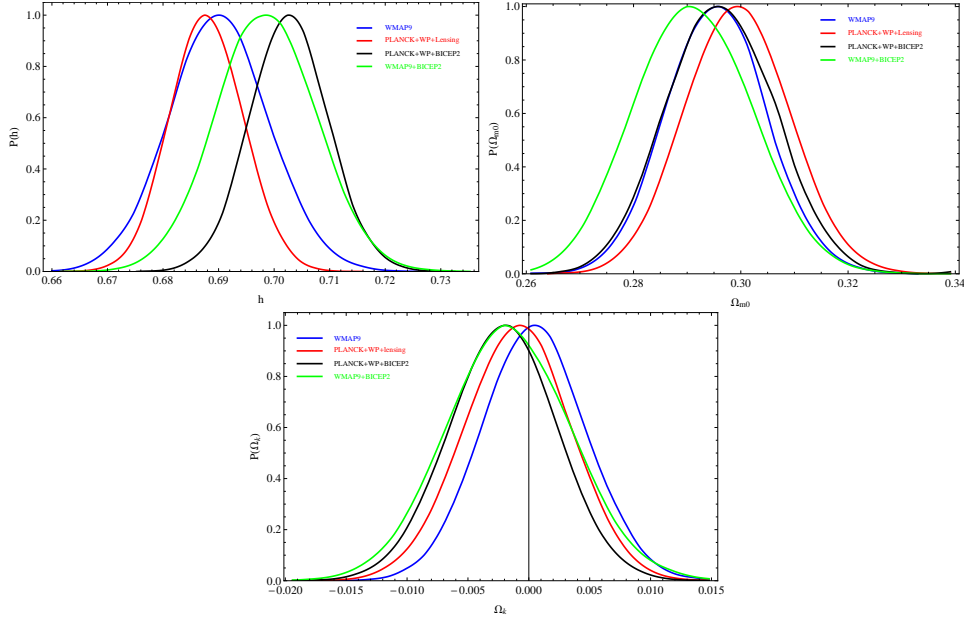


Fig. 2: Marginalized posterior distributions for  $h$  (top left),  $\Omega_{m0}$  (top right) and  $\Omega_k$  (bottom) of the  $\Omega_k+\Lambda$ CDM model.

used the newly released BICEP2  $B$ -mode polarization data together with the WMAP9 and Planck data to derive the reduced CMB data. We have found that the Planck data give tighter constraints on  $\{l_A, R, z_*$  than WMAP9 in the same cosmological model. While including the BICEP2 data, the standard deviations seem to be larger because of additional free parameters, the tensor-to-scalar ratio and running of the scalar spectral index.

We have combined these reduced CMB data with low-redshift observational data to constrain the cosmological parameters for the  $\Lambda$ CDM model and the  $w$ CDM model. The reduced CMB data from Planck+WP do not lead to significant improvement to the constraint on dark energy together with low-redshift observational data, compared to the reduced CMB

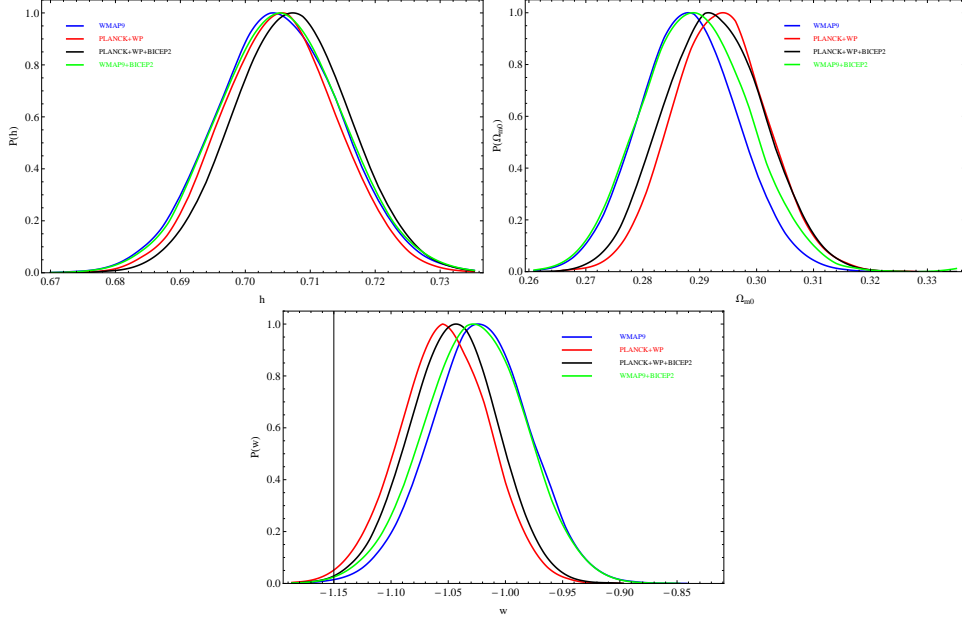


Fig. 3: Marginalized posterior distributions for  $h$  (top left),  $\Omega_{m0}$  (top right) and  $w$  (bottom) of the flat  $w$ CDM model.

data from WMAP9. Including BICEP2 data results in a higher value of the Hubble constant especially when the equation of state of dark energy and curvature are allowed to vary. For the  $\Omega_k + \Lambda$ CDM model, the constraint from Planck+WP+Lensing in combination with low-redshift observations gives  $h = 0.6880^{+0.0090}_{-0.0096}$ , which is inconsistent with the value of  $h = 0.7032^{+0.0106}_{-0.0113}$  derived from Planck+WP+BICEP2 at about  $1.3 \sigma$  CL. The constraint on  $w$  with Planck+WP gives  $w = -1.0507^{+0.0469}_{-0.0507}$ , favoring the phantom region at  $1 \sigma$  CL, for a flat  $w$ CDM model. The constraint on  $w$  with WMAP9 or Planck+WP+BICEP2 is consistent with  $w = -1$ . We have also found that the constraints on the cosmological parameters are not sensitive to the choice of the reduced CMB data derived from different cosmological models.

### Acknowledgments

This work was supported in part by the National Natural Science Foundation of China (No.10821504, No.10975168, No.11035008, No.11175225 and No.11335012), and in part by the Ministry of Science and Technology of China under Grant No. 2010CB833004 and No. 2010CB832805. RGC is also supported by the Strategic Priority Research Program

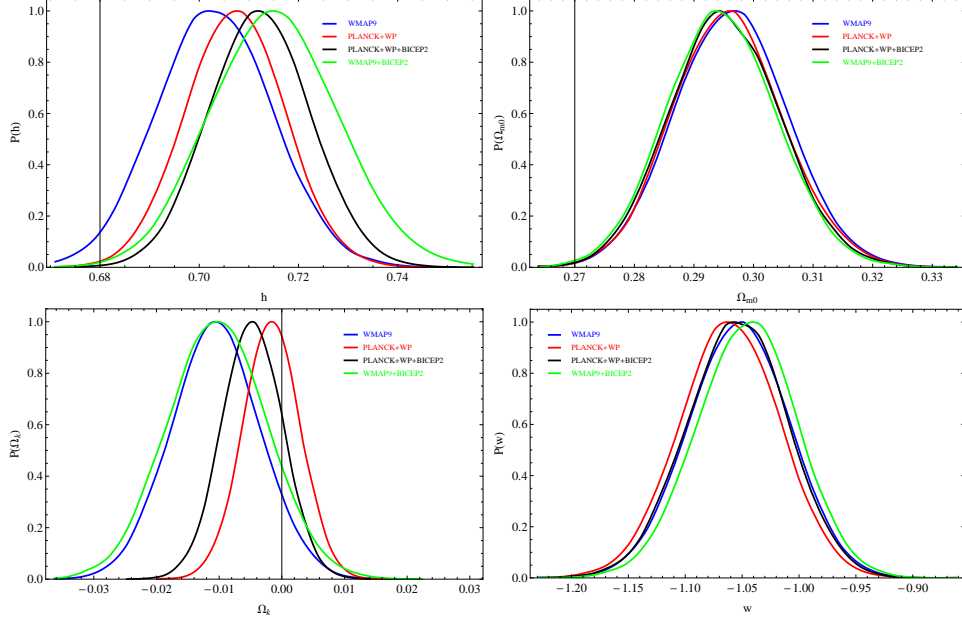


Fig. 4: Marginalized posterior distributions for  $h$  (top left),  $\Omega_{m0}$  (top right),  $\Omega_k$  (bottom left) and  $w$  (bottom right) of the  $\Omega_k+w$ CDM model.

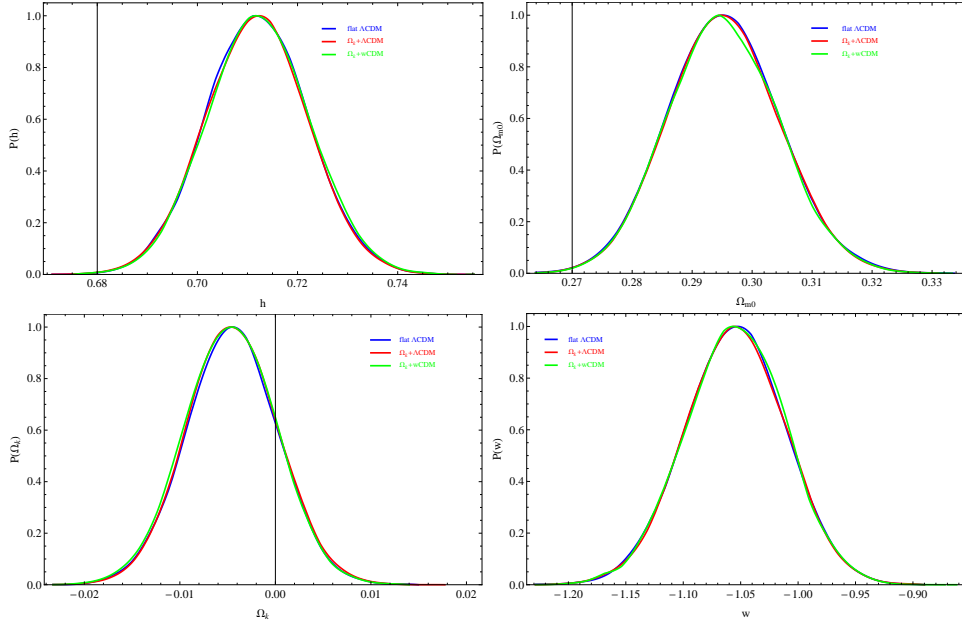


Fig. 5: Marginalized posterior distributions for  $h$  (top left),  $\Omega_{m0}$  (top right),  $\Omega_k$  (bottom left) and  $w$  (bottom right) of the  $\Omega_k+w$ CDM model from Planck+WP+BICEP2. Different colors correspond to the different models used to derive the reduced CMB data from Planck+WP+BICEP2.

The Emergence of Cosmological Structures of the Chinese Academy of Sciences, Grant No. XDB09000000. We used CosmoMC and CAMB. We acknowledge the use of the WMAP, Planck and BICEP2 data and the Lenovo DeepComp 7000 supercomputer in SCCAS.

# Appendices

## A. Type Ia Supernovae

In this work, we take the Union2.1 compilation [7], which contains 580 SNe Ia data over the redshift range  $0.015 \leq z \leq 1.414$ . The chisquare is defined as

$$\chi_{SN}^2 = \sum_{i=1}^{580} \frac{[\mu^{obs}(z_i) - \mu^{th}(z_i)]^2}{\sigma_{SN}^2(z_i)}, \quad (10)$$

where  $\mu^{obs}(z)$  is the measured distance modulus from the data and  $\mu^{th}(z)$  is the theoretical distance modulus, defined as

$$\mu^{th}(z) = 5 \log_{10} d_L + \mu_0, \quad \mu_0 = 42.384 - 5 \log_{10} h. \quad (11)$$

The luminosity distance is

$$d_L(z) = (1+z)r(z), \quad (12)$$

where  $r(z)$  is the comoving distance defined in equation (1). The nuisance parameter  $\mu_0$  can be eliminated by expanding  $\chi^2$  with respect to  $\mu_0$  as [34] :

$$\chi_{SN}^2 = A + 2B\mu_0 + C\mu_0^2, \quad (13)$$

where

$$\begin{aligned} A &= \sum_{i=1}^N \frac{[\mu^{th}(z_i; \mu_0 = 0) - \mu^{obs}(z_i)]^2}{\sigma_{SN}^2(z_i)}, \\ B &= \sum_{i=1}^N \frac{\mu^{th}(z_i; \mu_0 = 0) - \mu^{obs}(z_i)}{\sigma_{SN}^2(z_i)}, \\ C &= \sum_{i=1}^N \frac{1}{\sigma_{SN}^2(z_i)}. \end{aligned} \quad (14)$$

The  $\chi_{SN}^2$  has a minimum as

$$\tilde{\chi}_{SN}^2 = A - B^2/C, \quad (15)$$

In this way the nuisance parameter  $\mu_0$  is removed. This technique is equivalent to performing a uniform marginalization over  $\mu_0$  [34]. We will adopt  $\tilde{\chi}_{SN}^2$  as the goodness of fitting instead of  $\chi_{SN}^2$ .

## B. Observational Hubble parameter (HUB)

In this paper we use 19 observational Hubble data over the redshift range:  $0.07 \leq z \leq 2.3$ , which contain 11 observational Hubble data obtained from the differential ages of passively evolving galaxies [27, 32], and 8  $H(z)$  data at eight different redshifts obtained from the differential spectroscopic evolution of early type galaxies as a function of redshift [33]. The chisquare is defined as

$$\chi_{HUB}^2 = \sum_{i=1}^N \frac{[H_{th}(z_i) - H_{obs}(z_i)]^2}{\sigma_H^2(z_i)}, \quad (16)$$

where  $H_{th}(z)$  and  $H_{obs}(z)$  are the theoretical and observed values of Hubble parameter, and  $\sigma_H$  denotes the error of observed data.

## C. Baryon Acoustic Oscillation (BAO)

Baryon Acoustic Oscillation provides an efficient method for measuring the expansion history of the universe by using features in the cluster of galaxies with large scale survey. Here we use the results from the following five BAO surveys: the 6dF Galaxy Survey, SDSS DR7, SDSS DR9, WiggleZ measurements and the radial BAO measurement.

### 1. 6dF Galaxy Survey

The 6dFGS BAO detection can constrain the distance-redshift relation at  $z_{eff} = 0.106$  [38]. it gives a measurement of the distance ratio

$$\frac{r_s(z_d)}{D_V(z = 0.106)} = 0.336 \pm 0.015, \quad (17)$$

where  $r_s(z_d)$  is the comoving sound horizon at the baryon drag epoch when baryons became dynamically decoupled from photons. The redshift  $z_d$  is well approximated by [39]

$$z_d = \frac{1291(\Omega_{m0}h^2)^{0.251}}{1 + 0.659(\Omega_{m0}h^2)^{0.828}}[1 + b_1(\Omega_{b0}h^2)^{b_2}], \quad (18)$$

where

$$\begin{aligned} b_1 &= 0.313(\Omega_{m0}h^2)^{-0.419}[1 + 0.607(\Omega_{m0}h^2)^{0.674}], \\ b_2 &= 0.238(\Omega_{m0}h^2)^{0.223}. \end{aligned} \tag{19}$$

The effective ‘‘volume’’ distance  $D_V$  is a combination of the angular-diameter distance  $D_A(z)$  and the Hubble parameter  $H(z)$ ,

$$\begin{aligned} D_V(z) &= \left[ (r(z))^2 \frac{z}{H(z)} \right]^{1/3} \\ &= [(1+z)^2 D_A(z)^2 \frac{z}{H(z)}]^{1/3}. \end{aligned} \tag{20}$$

The  $\chi_{6dF}^2$  is defined by

$$\chi_{6dF}^2 = \frac{[(r_s(z_d)/D_V(0.106))_{th} - 0.336]^2}{0.015^2}. \tag{21}$$

## 2. SDSS DR7

The joint analysis of the 2-degree Field Galaxy Redshift Survey data and the Sloan Digital Sky Survey Data Release 7 data gives the distance ratio at  $z = 0.2$  and  $z = 0.35$  [40]:

$$\begin{aligned} \frac{r_s(z_d)}{D_V(z = 0.2)} &= 0.1905 \pm 0.0061, \\ \frac{r_s(z_d)}{D_V(z = 0.35)} &= 0.1097 \pm 0.0036. \end{aligned} \tag{22}$$

By applying the reconstruction technique [41] to the clustering of galaxies from the SDSS DR7 Luminous Red Galaxies sample, and sharpening the BAO feature, Padmanabhan *et al.* obtained the distance ratio at  $z = 0.35$  [42]:

$$\frac{r_s(z_d)}{D_V(z = 0.35)} = 0.1126 \pm 0.0022. \tag{23}$$

The SDSS DR7 and SDSS DR7 reanalysis results are based on the same survey and the latter gives a higher precision than the former, we therefore take the SDSS DR7 reanalysis data instead of the first one. The  $\chi_{DR7-re}^2$  used in the Markov Chain Monte Carlo analysis is

$$\chi_{DR7re}^2 = \frac{[(\frac{r_s(z_d)}{D_V(0.35)})_{th} - 0.1126]^2}{0.0022^2}. \tag{24}$$

### 3. SDSS DR9

The SDSS DR9 measurement gives the distance ratio at  $z = 0.57$  [43]:

$$\frac{r_s(z_d)}{D_V(z = 0.57)} = 0.0732 \pm 0.0012. \quad (25)$$

The chisquare here is defined as

$$\chi_{DR9}^2 = \frac{[(\frac{r_s(z_d)}{D_V(0.57)})_{th} - 0.0732]^2}{0.0012^2}. \quad (26)$$

### 4. The WiggleZ measurements

The WiggleZ team measures the acoustic parameter by encoding some shape information on the power spectrum [44]:

$$A(z) = \frac{D_V(z)\sqrt{\Omega_{m0}H_0}}{z}. \quad (27)$$

The baryon acoustic peaks measured at redshifts  $z = 0.44$ ,  $0.6$  and  $0.73$  in the galaxy correlation function of the final dataset of the WiggleZ Dark Energy Survey give

$$\begin{aligned} A(z = 0.44) &= 0.474 \pm 0.034, \\ A(z = 0.60) &= 0.442 \pm 0.020, \\ A(z = 0.73) &= 0.424 \pm 0.021. \end{aligned} \quad (28)$$

The corresponding chisquare is defined as

$$\chi_{Wig}^2 = X^T V^{-1} X, \quad (29)$$

where

$$X = \begin{bmatrix} A(z = 0.44)_{th} - 0.474 \\ A(z = 0.60)_{th} - 0.442 \\ A(z = 0.73)_{th} - 0.424 \end{bmatrix}, \quad (30)$$

and its inverse covariance matrix is

$$V^{-1} = \begin{bmatrix} 1040.3 & -807.5 & 336.8 \\ -807.5 & 3720.3 & -1551.9 \\ 336.8 & -1551.9 & 2914.9 \end{bmatrix}. \quad (31)$$

## 5. Radial BAO

The radial (line-of-sight) baryon acoustic scale can also be measured by using the SDSS data. It is independent from the BAO measurements described above. The measured quantity is

$$\Delta_z(z) = H(z)r_s(z_d), \quad (32)$$

whose values are given by [45] as

$$\begin{aligned} \Delta_z(0.24) &= 0.0407 \pm 0.0011, \\ \Delta_z(0.43) &= 0.0442 \pm 0.0015. \end{aligned} \quad (33)$$

### D. Reduced CMB data

The chisquare for the reduced CMB data is defined by

$$\chi_{CMB}^2 = X^T C^{-1} X, \quad (34)$$

where

$$X = \begin{bmatrix} (l_A)_{th} - (l_A)_{obs} \\ R_{th} - R_{obs} \\ (z_*)_{th} - (z_*)_{obs}, \end{bmatrix} \quad (35)$$

and  $C$  is the related covariance matrix.

- 
- [1] A. G. Riess *et al.* [Supernova Search Team Collaboration], *Astron. J.* **116**, 1009 (1998) [astro-ph/9805201].
  - [2] S. Perlmutter *et al.* [Supernova Cosmology Project Collaboration], *Astrophys. J.* **517**, 565 (1999) [astro-ph/9812133].
  - [3] E. Komatsu *et al.* [WMAP Collaboration], *Astrophys. J. Suppl.* **192**, 18 (2011) [arXiv:1001.4538 [astro-ph.CO]].
  - [4] Y. Wang and P. Mukherjee, *Phys. Rev. D* **76**, 103533 (2007) [astro-ph/0703780].
  - [5] Y. Wang and S. Wang, *Phys. Rev. D* **88**, 043522 (2013) [arXiv:1304.4514 [astro-ph.CO]].
  - [6] D. L. Shafer and D. Huterer, *Phys. Rev. D* **89**, 063510 (2014) [arXiv:1312.1688 [astro-ph.CO]].
  - [7] N. Suzuki *et al.*, *Astrophys. J.* **746**, 85 (2012) [arXiv:1105.3470 [astro-ph.CO]].

- [8] A. Conley *et al.* [SNLS Collaboration], *Astrophys. J. Suppl.* **192**, 1 (2011) [arXiv:1104.1443 [astro-ph.CO]].
- [9] A. Rest, D. Scolnic, R. J. Foley, M. E. Huber, R. Chornock, G. Narayan, J. L. Tonry and E. Berger *et al.*, arXiv:1310.3828 [astro-ph.CO].
- [10] Q. Su, Z. L. Tuo and R. G. Cai, *Phys. Rev. D* **84**, 103519 (2011) [arXiv:1109.2846 [astro-ph.CO]].
- [11] R. G. Cai, Z. K. Guo and B. Tang, *Phys. Rev. D* **89**, 123518 (2014) [arXiv:1312.4309 [astro-ph.CO]].
- [12] Q. Gao and Y. Gong, *Class. Quant. Grav.* **31**, 105007 (2014) [arXiv:1308.5627 [astro-ph.CO]].
- [13] Y. Zhang and Y. Gong, arXiv:1306.6663 [astro-ph.CO].
- [14] P. S. Corasaniti and A. Melchiorri, *Phys. Rev. D* **77**, 103507 (2008) [arXiv:0711.4119 [astro-ph]].
- [15] G. Hinshaw *et al.* [WMAP Collaboration], *Astrophys. J. Suppl.* **208**, 19 (2013) [arXiv:1212.5226 [astro-ph.CO]].
- [16] P. A. R. Ade *et al.* [Planck Collaboration], arXiv:1303.5076 [astro-ph.CO].
- [17] P. A. R. Ade *et al.* [BICEP2 Collaboration], *Phys. Rev. Lett.* **112**, 241101 (2014) [arXiv:1403.3985 [astro-ph.CO]].
- [18] G. Mangano, G. Miele, S. Pastor, T. Pinto, O. Pisanti and P. D. Serpico, *Nucl. Phys. B* **729**, 221 (2005) [hep-ph/0506164].
- [19] W. Hu and N. Sugiyama, *Astrophys. J.* **471**, 542 (1996) [astro-ph/9510117].
- [20] A. Lewis and S. Bridle, *Phys. Rev. D* **66**, 103511 (2002) [astro-ph/0205436].
- [21] B. Hu, J. W. Hu, Z. K. Guo and R. G. Cai, *Phys. Rev. D* **90**, 023544 (2014) [arXiv:1404.3690].
- [22] M. J. Mortonson and U. Seljak, *JCAP* **1410**, no. 10, 035 (2014) [arXiv:1405.5857 [astro-ph.CO]].
- [23] R. Flauger, J. C. Hill and D. N. Spergel, *JCAP* **1408**, 039 (2014) [arXiv:1405.7351 [astro-ph.CO]].
- [24] R. Adam *et al.* [Planck Collaboration], arXiv:1409.5738 [astro-ph.CO].
- [25] K. Tassis and V. Pavlidou, arXiv:1410.8136 [astro-ph.CO].
- [26] W. N. Colley and J. R. Gott, arXiv:1409.4491 [astro-ph.CO].
- [27] D. Stern, R. Jimenez, L. Verde, M. Kamionkowski and S. A. Stanford, *JCAP* **1002**, 008 (2010) [arXiv:0907.3149 [astro-ph.CO]].

- [28] A. G. Riess, L. Macri, S. Casertano, H. Lampeitl, H. C. Ferguson, A. V. Filippenko, S. W. Jha and W. Li *et al.*, *Astrophys. J.* **730**, 119 (2011) [Erratum-ibid. **732**, 129 (2011)] [arXiv:1103.2976 [astro-ph.CO]].
- [29] W. L. Freedman, B. F. Madore, V. Scowcroft, C. Burns, A. Monson, S. E. Persson, M. Seibert and J. Rigby, *Astrophys. J.* **758**, 24 (2012) [arXiv:1208.3281 [astro-ph.CO]].
- [30] Z. Li, P. Wu, H. Yu and Z. -H. Zhu, *Sci. China Phys. Mech. Astron.* **57**, 381 (2014) [arXiv:1311.3467 [astro-ph.CO]].
- [31] G. Efstathiou, arXiv:1311.3461 [astro-ph.CO].
- [32] J. Simon, L. Verde and R. Jimenez, *Phys. Rev. D* **71**, 123001 (2005) [astro-ph/0412269].
- [33] M. Moresco, A. Cimatti, R. Jimenez, L. Pozzetti, G. Zamorani, M. Bolzonella, J. Dunlop and F. Lamareille *et al.*, *JCAP* **1208**, 006 (2012) [arXiv:1201.3609 [astro-ph.CO]].
- O. Farooq and B. Ratra, *Astrophys. J.* **766**, L7 (2013) [arXiv:1301.5243 [astro-ph.CO]].
- [34] S. Nesseris and L. Perivolaropoulos, *Phys. Rev. D* **72**, 123519 (2005) [astro-ph/0511040].
- [35] V. Sahni, *Class. Quant. Grav.* **19**, 3435 (2002) [astro-ph/0202076].
- [36] T. Padmanabhan, *Phys. Rept.* **380**, 235 (2003) [hep-th/0212290].
- [37] N. Suzuki, D. Rubin, C. Lidman, G. Aldering, R. Amanullah, K. Barbary, L. F. Barrientos and J. Botyanszki *et al.*, *Astrophys. J.* **746**, 85 (2012) [arXiv:1105.3470 [astro-ph.CO]].
- [38] F. Beutler, C. Blake, M. Colless, D. H. Jones, L. Staveley-Smith, L. Campbell, Q. Parker and W. Saunders *et al.*, *Mon. Not. Roy. Astron. Soc.* **416**, 3017 (2011) [arXiv:1106.3366 [astro-ph.CO]].
- [39] D. J. Eisenstein and W. Hu, *Astrophys. J.* **496**, 605 (1998) [astro-ph/9709112].
- [40] W. J. Percival *et al.* [SDSS Collaboration], *Mon. Not. Roy. Astron. Soc.* **401**, 2148 (2010) [arXiv:0907.1660 [astro-ph.CO]].
- [41] D. J. Eisenstein, H. -j. Seo, E. Sirko and D. Spergel, *Astrophys. J.* **664**, 675 (2007) [astro-ph/0604362].
- [42] N. Padmanabhan, X. Xu, D. J. Eisenstein, R. Scalzo, A. J. Cuesta, K. T. Mehta and E. Kazin, *Mon. Not. Roy. Astron. Soc.* **427**, no. 3, 2132 (2012) [arXiv:1202.0090 [astro-ph.CO]].
- [43] L. Anderson, E. Aubourg, S. Bailey, D. Bizyaev, M. Blanton, A. S. Bolton, J. Brinkmann and J. R. Brownstein *et al.*, *Mon. Not. Roy. Astron. Soc.* **427**, no. 4, 3435 (2013) [arXiv:1203.6594 [astro-ph.CO]].
- [44] C. Blake, E. Kazin, F. Beutler, T. Davis, D. Parkinson, S. Brough, M. Colless and C. Contreras

- et al.*, Mon. Not. Roy. Astron. Soc. **418**, 1707 (2011) [arXiv:1108.2635 [astro-ph.CO]].
- [45] E. Gaztanaga, R. Miquel and E. Sanchez, Phys. Rev. Lett. **103**, 091302 (2009) [arXiv:0808.1921 [astro-ph]].